Talukder Z. Jubery
Prashanta Dutta

School of Mechanical and Materials Engineering, Washington State University, Pullman, Washington, USA

Received October 14, 2012
Revised December 6, 2012
Accepted December 6, 2012

Research Article

A new design for efficient dielectrophoretic separation of cells in a microdevice

Effectiveness of a continuous biological cell separation device can be improved significantly by increasing the distance among different types of cells. To achieve this, most of the recent dielectrophoresis based continuous separation devices implement differential forces on cells either along the transverse direction or the vertical direction with respect to the bulk fluid flow motion. However, interparticle distance can be increased further by implementing forces along both transverse and vertical planes. In this article, a design for a microfluidic platform has been proposed where a new electrode configuration is identified to implement symmetric forces in both vertical and transverse directions. A numerical model, which considers presence of particles in the electric field and flow field, shows a much higher interparticle distance between red blood cells and plasmodium falciparum infected red blood cells in such a device than that in a conventional separation device. This configuration also reduces the possibility of particle trapping on the electrodes, which is a major bottleneck of dielectrophoresis.

Keywords:
Dielectrophoresis / Electrode design / Microfluidic / Particle separation
DOI 10.1002/elps.201200560

Additional supporting information may be found in the online version of this article at the publisher's web-site

1 Introduction

DEP is the motion of a dielectric particle in a spatially nonuniform electric field [1]. It can be used on both charged and insulating particles to move them selectively in a liquid medium. The magnitude and direction of dielectrophoretic forces depend on the relative polarizability of the particle and the surrounding liquid. If the particle is less polarizable than the surrounding liquid, the particle will move toward the lower electric field region which is known as negative DEP. On the other hand, in positive DEP particle is more polarizable than the medium and particle migrates toward the higher electric field region [2].

DEP is an effective tool for separation of biological particles such as cells, bacteria, virus, etc. for biomedical and biotechnological applications. DEP-based particle separation can be achieved in two different ways: discontinuous and continuous. In both types, an appropriate fluid flow is introduced along the longitudinal (axial) direction in addition to the nonuniform electric fields. In the discontinuous method [3, 4] a mixture of particles suspended in a buffer solution is allowed to flow through a microdevice, and target cells are selectively trapped on the predefined locations generally on electrode surfaces by positive DEP. On the other hand, in continuous dielectrophoretic separation [5], target and unwanted particles are collected separately in two different outlets. This can be achieved by applying mode variation [6, 7] or magnitude change [5, 8] in the dielectrophoretic force. In mode variation, target particles experience one mode of DEP (negative or positive), whereas unwanted particles are subjected to the opposite mode of DEP. Thus, particles deviate from their original trajectories in two different directions: toward electrodes in the high electric field region (positive DEP) or away from the electrodes toward low electric field region (negative DEP). The positive DEP mode is generally optimized with the fluid flow so that particles do not trap at or near electrodes but move along with the flow field. Therefore, both types of particles can be collected at their respective outlets.

The magnitude variation-based continuous separation only uses negative DEP. In this method, different types of particles are levitated at different heights or repelled to

Correspondence: Dr. Prashanta Dutta, School of Mechanical and Materials Engineering, Washington State University, Pullman, Washington 99164-2920, USA
E-mail: dutta@mail.wsu.edu
Fax: +1-509-335-4662

Abbreviations: PF, plasmodium falciparum; **RBC**, red blood cell

Colour Online: See the article online to view Fig. 1–6 in colour.

different lateral positions [9–11] based on their size and dielectric properties, and then allowed them to flow through the separation channel before being collected at different outlets. This magnitude variation-based continuous separation is preferable in bioparticle separation because most physiological media including the whole blood have high conductivities, where cells become less polarizable than the medium, resulting in an effective negative DEP forces on them. Also in this type of separation, cells do not come close to the high electric field region and thus are not subjected to adverse effects such as dielectric breakdown, shear deformation, Joule heating, etc.

In continuous dielectrophoretic separation, the efficiency of the device depends on the interparticle distance between the target and unwanted particles. Various parameters were optimized to increase the separation efficiency such as electrode configurations [12, 13], flow rate [14], applied AC frequency [12, 15, 16], medium conductivity [6], applied electric potential [17], etc. In most of these devices, particles of interest are deviated from their original traveling (bulk fluid flow) path by implementing a dielectrophoretic force in either vertical [8] or transverse direction. However, it is very challenging to separate particles of same size and shape and very similar dielectric properties using one directional force. For example, when a cell is infected by virus, the size and shape of the cell remain the same as healthy cell, but their dielectric properties such as conductivity (σ) and permittivity (ε) change only slightly due to the viral infection [18]. In this scenario, a better way to increase the separation between the healthy and infected cell is by introducing forces in both vertical and transverse directions.

In literature, there exist a number of studies demonstrating the dielectrophoretic forces in two directions using extruded electrodes [19, 20] and top and bottom wall-angled electrodes [21, 22]. Iliescu et al. [20] have used extruded rectangular electrodes to separate viable and nonviable yeast cell by trapping them at specific locations. Therefore, their electrode configuration is not suitable for continuous DEP separation. On the other hand, Dürr et al. [21] have shown angular electrodes to create 2D dielectrophoretic force in a microdevice for separation of synthetic microparticles. However, their configuration only provides significant force in transverse direction, and thus particle displacement is primarily in the transverse direction. One can increase the magnitude of the DEP force to improve the separation, but the maximum DEP force that can be applied at a particular direction is limited by the dielectric breakdown and shear deformation.

Application of symmetric dielectrophoretic forces has the potential to maximize the separation distance between particles. In other words, to maintain a particular separation distance, the magnitude of the dielectrophoretic force will be minimum if forces are applied symmetrically in both vertical and transverse planes. However, no previous work has shown a systematic study to improve the effectiveness of separation using symmetric dielectrophoretic forces. Thus, the objective of this article is to design a microdevice to demonstrate the possibility of symmetric dielectrophoretic forces on particles for better separation by introducing an innovative electrode design. The main goal of this new electrode design is to apply significant dielectrophoretic forces in both transverse and vertical directions with respect to the bulk fluid flow. This eventually can create higher interparticle separation in smaller space with comparatively low applied electric field value, and will be suitable for separation of particles of very close dielectric properties.

2 Materials and methods

2.1 Mathematical model and numerical method

In a DEP-based continuous separation device, the particles are suspended in a fluid medium. In a microfluidic device, the size of the particles becomes comparable to the device domain, and thus one has to consider the size of the particles in calculating the dielectrophoretic forces acting on particles. Let us assume that the entire device domain (Ω) is consisted of solid/particle domains ($\Omega_s(t)$) and a fluid domain ($\Omega_f(t)$). The interface between the solid and the fluid domains is denoted by $\partial\Omega_s(t)$ and other boundaries are given as $\partial\Omega$. A biological cell can be considered as a single solid particle of homogenous properties using single shell model [23, 24]. Therefore, the properties within the cell can be assumed constant in the analysis.

Using distributed Lagrange multiplier formulation [25], the velocity field for the whole domain (Ω) can be expressed with the following unified equations:

$$\rho\left(\frac{\partial \vec{V}}{\partial t} + (\vec{V}\cdot\vec{\nabla})\vec{V}\right) = -\nabla p + \mu\nabla^2\vec{V} + \rho g + (1-d_h)\vec{f}_{bf} + d_h(\vec{f}_{bs} + \vec{f}_{ps}) \text{ in } \Omega, \quad (1)$$

$$\nabla\cdot\vec{V} = 0 \qquad \text{in } \Omega, \quad (2)$$

$$\nabla\cdot D[\vec{V}] = 0 \qquad \text{in } \Omega_s(t) \quad (3)$$

$$D[\vec{V}]\cdot\vec{n} = 0 \qquad \text{in } \partial\Omega_s(t) \quad (4)$$

where ρ_f, μ, $\vec{V}$, and p are the fluid density, viscosity, velocity, and pressure, respectively; g is the gravitational acceleration; $\vec{f}_{bf}$, $\vec{f}_{bs}$, and $\vec{f}_{ps}$ are the electrical body force on fluid, electrical body force on solid, and an extra force on solid, respectively. $D[\vec{V}]$ is the rate of strain tensor, d_h is the indicator function that assumes 1 in $\Omega_s(t)$ and 0 in $\Omega_f(t)$. The unified density can be expressed as:

$$\rho = (1-d_h)\rho_f + d_h\rho_s \quad (5)$$

where ρ_s is the particle density. Using complex variables formulation, governing equations for electric potential ($\tilde{\phi}$) in an AC DEP can be written as:

$$\nabla\cdot(\tilde{\varepsilon}\nabla\tilde{\phi}) = 0 \qquad \text{in } \Omega \quad (6)$$

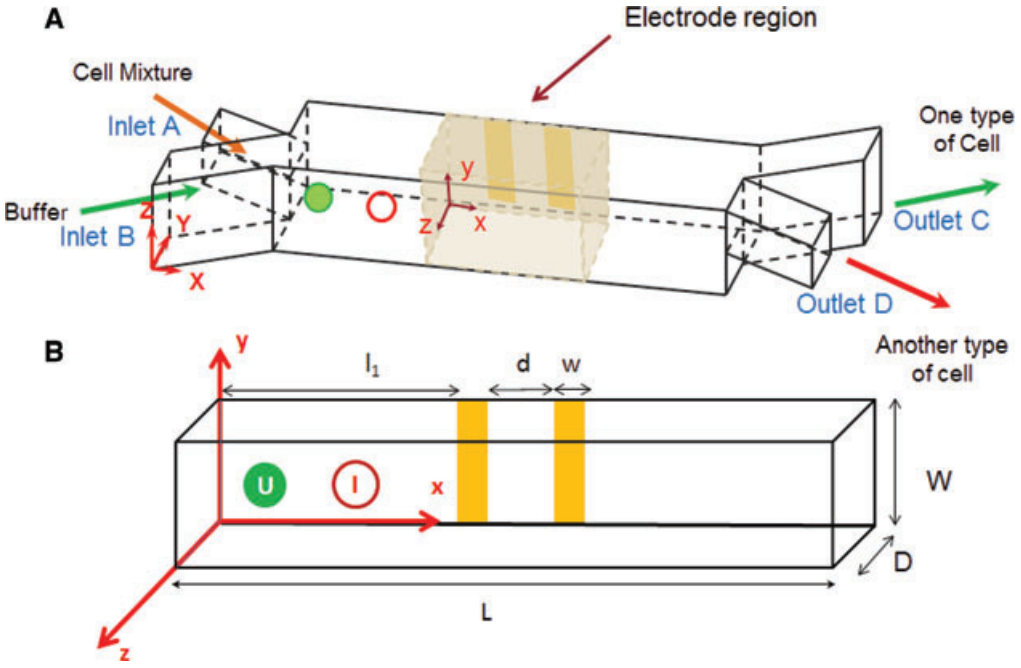

Figure 1. (A) Schematic of the proposed separation device containing cells. The device has two inlets: inlet A and inlet B, and two outlets: outlet C and outlet D. Heights of inlet A and inlet B are 20 and 40 μm, respectively. A mixture of cells is introduced through inlet A and buffer is introduced through inlet B. The bulk fluid flow velocity through these inlets is 200 μm/s. The heights of outlet C and D are 40 and 20 μm, respectively. (B) Computational domain for simulation-considering particles. This domain is considered from the shaded region in the actual device. The length, width, and height of the separation channel are (L), (D), and (W), respectively, and electrodes are shown on the back wall only. Here local coordinate system x-y-z has been used for the convenience of presentation.

where $\tilde{\varepsilon}$ is the unified complex permittivity which is given as $\tilde{\varepsilon} = d_h \cdot \tilde{\varepsilon}_s + (1 - d_h) \cdot \tilde{\varepsilon}_f$, and $\tilde{\varepsilon}_s = \varepsilon_s - \frac{i\sigma_s}{\omega}$ and $\tilde{\varepsilon}_f = \varepsilon_f - \frac{i\sigma_f}{\omega}$ are the complex permittivity of solid and fluid, respectively. The angular frequency ω is related to applied electric frequency f as $\omega = 2\pi f$.

The time averaged electrical body force in the solid domain can be expressed as [26]:

$$\vec{f}_{bs} = \frac{\varepsilon}{4}\nabla \cdot (\tilde{\vec{E}}\,\tilde{\vec{E}}^{*} + \tilde{\vec{E}}^{*}\,\tilde{\vec{E}} - |\tilde{\vec{E}}|^2 \vec{I}) \quad \text{in } \Omega_s(t) \tag{7}$$

where $\tilde{\vec{E}}$ is the complex electric field that is related to the complex electric potential ($\tilde{\phi}$) by $\tilde{\vec{E}} = -\nabla\tilde{\phi}$. $\tilde{\vec{E}}^{*}$ is complex conjugate of electric field $\tilde{\vec{E}}$. In this study, we neglect electroosmotic and electrophoretic forces due to the applied AC electric field.

2.2 Proposed microdevice and boundary conditions

Figure 1A shows the schematic of proposed microfluidic platform for continuous cell separation. The device has two inlets: inlet A and inlet B, and two outlets: outlet C and outlet D. A mixture of cells is introduced in the main channel through the inlet A, and buffer is introduced through the inlet B. To control the entry of the cell mixture, the height of the inlet A is considered to be the half of the separation channel. Cells' trajectories will be altered by applying electric potential difference between electrodes located at the wall(s) of microchannel. The cells are collected through different outlets. Here, our objective is to keep different types of cells apart as much as possible. This can be achieved if one type of cell is directed toward the upper right section of the outlet, while the other type is close to the bottom left section. For that reason, the height of the outlet channel D was set as the half of the separation channel.

In this device, due to low Reynolds number creeping flow, the cells will follow the streamlines (not shown) of the fluid flow before reaching the electrode region. Since, particles will start deviating at the electrode region, a multidomain model is developed to predict particles' trajectories. A smaller domain (referred to as separation domain from this point forward) around the electrodes (Fig. 1B) is selected to accurately model the dielectrophoretic force acting on separation (dashed) region encompassing the electrodes. For the regular/whole domain (Fig. 1A), a specified velocity is considered at the inlets, and normal flow with $p = 0$ is used as the boundary condition for outlets. A no-slip velocity condition is assumed on all other solid boundaries. Flow boundary conditions for the separation domain (Fig. 1B) are obtained from the solution of the flow field in the regular domain without the presence of any particle [27]. In unified flow field model, we neglect the density variation between solid and fluid domains, as cytoplasm of a cell is generally comprised of liquid of the same density as the surrounding medium. For the unified electric potential equation (Eq. (6)), specified

Table 1. Dielectric properties of RBCs and PF-infected (PFI) RBCs [18]

	Membrane conductivity (S/m)	Membrane permittivity (F/m)	Cytoplasm conductivity (S/m)	Cytoplasm permittivity (F/m)
RBC	1.4e-6	60e-12	0.52	285e-12
PFI RBC	5.7e-6	50e-12	0.52	285e-12

electric potential is considered at electrodes and insulating boundary condition is maintained at all other boundaries for the regular domain. Like flow field, the boundary conditions for the electric potential in the separation domain come from the results of the whole domain simulation.

3 Results and discussion

The primary objective of this work is to develop a microfluidic platform for improving separation of cells via magnitude variation-based continuous DEP. The main feature of this device is to increase the interparticle distance by applying forces on particles in both transverse and vertical directions with respect to the bulk fluid flow direction. An in-house numerical model is developed based on finite volume method [28]. The detail of the numerical model is presented elsewhere [29], and a brief description of key features of this model is provided in Supporting Information materials.

Numerical simulation is performed to optimize various parameters such as electrode shape and electrode position for the proposed microfluidic platform (Fig. 1). In this study, both maximum width of an electrode and space between adjacent electrodes are kept constant as 30 μm. For design purpose only, straight- and trapezoidal-shaped electrodes are used, but our numerical model is capable of handling any shape of electrodes. To facilitate the device design process, we considered two types of cells: uninfected red blood cells (RBCs) and plasmodium falciparum (PF) infected RBCs. During the invasion of PF malaria parasite in the RBC, the RBC cells go through some physiological changes, which is responsible for slight changes in electrical properties of the cells. Table 1 shows the electrical properties of these two types of cells. In this study, cell diameter and membrane thickness are considered as 6 μm and 5 nm, respectively [30]; the buffer medium's relative permittivity and conductivity are set as 63 and 80 mS/m, respectively [31].

3.1 Selection of frequency

In magnitude variation-based DEP, particles are moved from the electrodes toward a lower electric field region by imposing a negative dielectrophoretic force. For a specified medium, the required frequency for negative dielectrophoretic force can be determined from the Clausius–Mossotti factor. For the system considered here, the real part of Clausius–Mossotti factor (See Supporting Information Fig. 1) reveals that the infected cell will have zero dielectrophoretic effect (i.e. Re [CMF] = 0) at applied frequency 495 kHz, while uninfected cell will attain the same condition at 375 kHz. Therefore, below 375 kHz both type of cells will experience negative dielectrophoretic force, and this force will be stronger for infected cell due to its higher absolute value of Re[CMF]. Thus, we have chosen 370 kHz for separation of these two types of cells in our proposed device.

3.2 Design of electrode shape and position

Electrode configuration is a vital parameter to apply dielectrophoretic forces effectively on the particles. In the proposed microdevice, bulk fluid flows in the x (longitudinal) direction. Thus, we would like to select an electrode configuration which will implement forces in both y (vertical) and z (transverse) directions on the cells. In this electrode design process, we are also examining the preferable condition for getting symmetric forces in both directions, which will maximize the interparticle distance. To achieve that, five different electrode configurations (Fig. 2) are considered on the wall(s) of the separation channel.

First, we consider only one cell, either uninfected or infected cell, in the separation domain to determine its trajectory in an applied AC electric field. In this case, conventional point-based method is applied to simulate the trajectory of the cell. It is important to note that, point-based method deviates from the actual results when particle is comparable to the domain or close to electrodes or close to other particle(s). However, it provides a qualitative idea, which is very useful for preliminary electrode design and selection process. Moreover, this method does not require solution of flow field or electric field in the presence of particle(s). Thus, it speeds up the electrode screening process.

The design process starts with a set of rectangular electrodes on the vertical wall (xy plane) of microdevice as shown in Fig. 2A. Numerical results show that this configuration will create a gradient of electric field in z direction, and a cell should experience force in transverse direction. To obtain the particle trajectory, the cells are initially considered at x = 10 μm, y = 10 μm, and z = 10 μm in the separation domain. The corresponding trajectories of infected and uninfected cells are shown in Figs. 3 and 4, respectively. As expected, the trajectories reveal that both cells experience only transverse (z) directional force. Although this configuration provides good separation between different types of cells, it cannot be used for the device configuration shown in Fig. 1. Moreover, due to the lack of the vertical directional force, particles might stick to the bottom wall if particles are introduced very close to the bottom wall of the channel.

Next, a set of trapezoidal electrodes is considered in xy plane instead of rectangular electrodes (Fig. 2B). Due to the gradual variation of width in y direction, this trapezoidal configuration will create a gradient of electric field in y direction in addition to electric field gradient in z-direction.

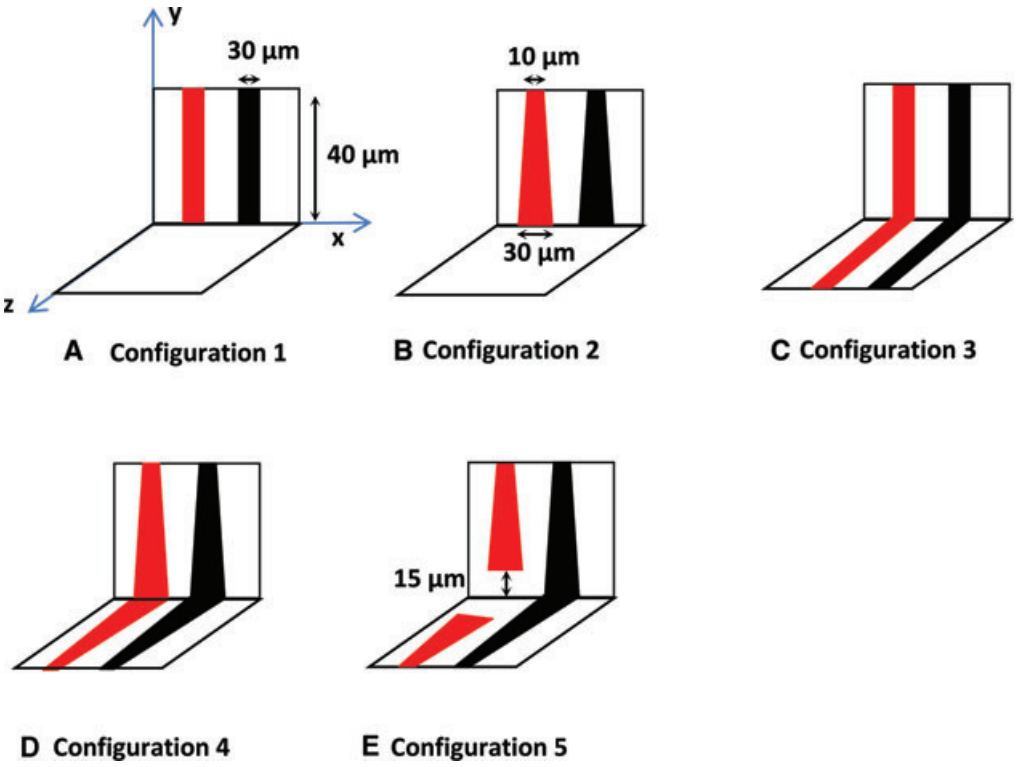

Figure 2. Configuration of electrodes considered for the design of the proposed separation microdevice. (A) Configuration 1: rectangular, (B) Configuration 2: trapezoidal, (C) Configuration 3: multiplane rectangular, (D) Configuration 4: multiplane trapezoidal, (E) Configuration 5: hybrid trapezoidal. Here red and black colors of the electrodes are used to differentiate the polarity of electrodes.

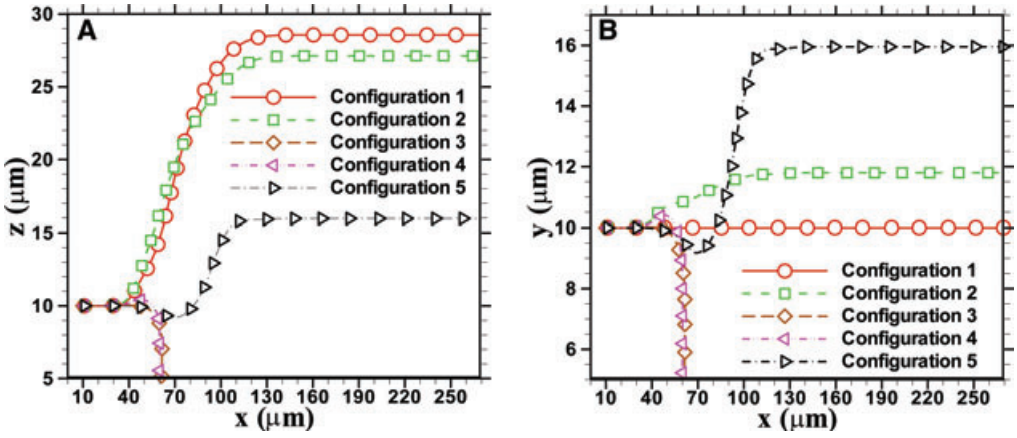

Figure 3. Effect of electrode configuration on cell displacement in transverse and vertical directions. (A) Levitation of infected (PF-infected RBCs) cells in z (transverse) direction, and (B) levitation of infected cell in y (vertical) direction. Particles are initially at x = 10 µm, y = 10 µm, and z = 10 µm. Here L = 350 µm, W = 40 µm, D = 40 µm, d = 30 µm, w = 30 µm, and l_1 = 40 µm. The applied electric potential difference between a pair of electrodes is 10 $V_{p\text{-}p}$ and inlet fluid velocity is found from the flow field solution of main domain as shown in Fig. 1A.

The trajectories (Figs. 3 and 4) indicate that both types of cells have a y directional motion along with z directional movement. However, the levitation/displacement in the y-direction is not the same as that in z-direction. We have also found that changing the dimension of trapezoidal electrodes between 10 to 30 µm has minor effect in the y directional displacement (See Supporting Information Fig. 2). It also suggests that it is difficult to generate symmetric electric field gradient in both y and z directions by only changing shape of trapezoidal electrodes. Therefore, for getting similar forcing and displacement effect on a cell in both y and z directions, a multiplane rectangular electrode configuration (where electrodes are in both xz and xy planes) is considered (Fig. 2C). For this electrode configuration, the uninfected cell

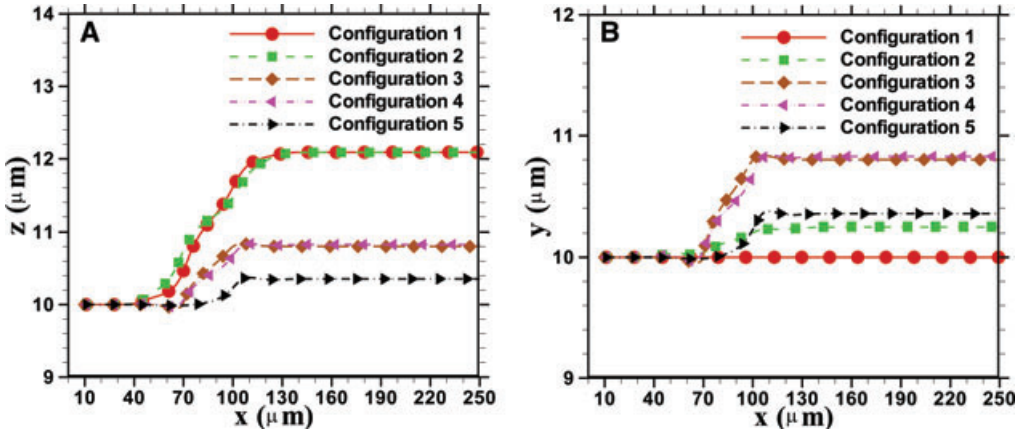

Figure 4. Effect of electrode configuration on cell displacement in transverse and vertical directions. (A) Levitation of uninfected RBCs in transverse direction, and (B) levitation of uninfected cells in vertical direction. Particles are initially at x = 10 μm, y = 10 μm, and z = 10 μm. The applied electric potential difference between a pair of electrodes is 10 $V_{p\text{-}p}$, inlet fluid velocity is found from the flow field solution of main domain as shown in Fig. 1A, and all other parameters are same as in Fig. 3.

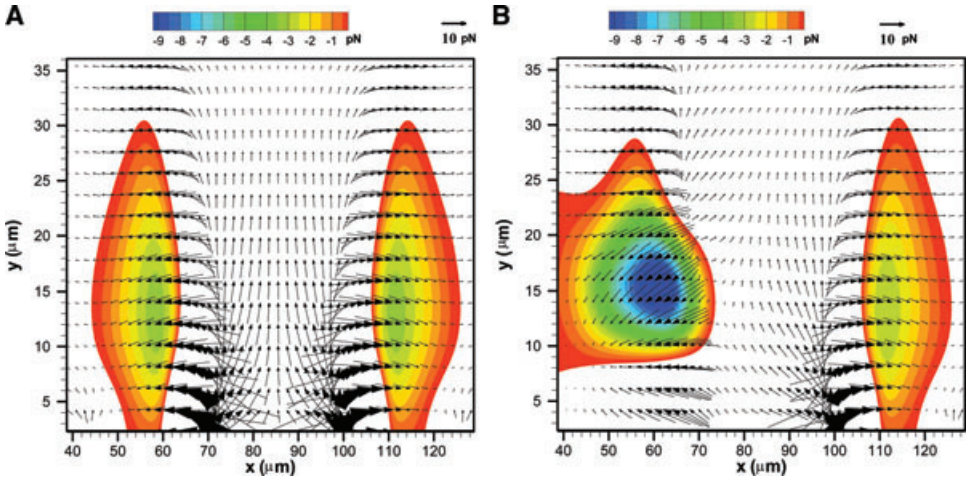

Figure 5. Dielectrophoretic force vectors and contour of only y directional force on the infected cell for (A) configuration 4 and (B) configuration 5 at a plane z = 10 μm. Due to symmetry of electrode configuration, identical force vectors are found at a plane of y = 10 μm. The x-location of the first electrode is between 40 and 70 μm, while the second electrode is located between 100 and 130 μm. The applied electric potential difference is 10 $V_{p\text{-}p}$.

displaces/levitates approximately 1 micron in both y and z directions as shown in Fig. 4, but the infected cell approaches toward the electrodes (Fig. 3) that is not desirable. Figure 3 also indicates that a multiplane trapezoidal electrode configuration (Fig. 2D) will produce the similar unacceptable results.

The contour of dielectrophoretic force on the infected cell (Fig. 5A) reveals that infected cell will experience negative y and z directional force while passing over the electrodes. This contour plot also shows that this configuration of electrodes create a region of low electric field near the corner where electrodes on the two planes (xy and xz) intersect. Consequently, as cell progresses in positive x direction due to bulk fluid flow, the value of dielectrophoretic force toward the electrodes will increase. Due to the higher value of Re[CMF], the negative dielectric force is stronger on infected cell than that on uninfected cell. For that reason, infected cell heads toward the electrodes, but the uninfected one can avoid the trapping in the electrode region as hydrodynamic force dominates over the weak negative dielectrophoretic force.

To circumvent the trapping of infected cells in the low electric field region at the intersection of electrodes, a hybrid trapezoidal configuration (Fig. 2E), consisting of a set of trapezoidal electrodes and a set of truncated trapezoidal electrodes, is considered. In this study, the truncation length was varied from 5 to 20 μm (not shown), and optimum levitation results are obtained for a truncation length of 10–15 μm. For hybrid trapezoidal electrode configuration (Fig. 2E), the infected cell first goes (Fig. 3) slightly toward electrodes (negative in y and z direction) and then moves away from electrodes (positive in y and z directions). Here the net displacement of infected cell in positive y and z directions is found approximately 6 μm, which was negative in the configurations 3 and 4.

Figure 5B reveals that while passing over the first set of electrodes an infected cell will try to reach around y = 8 μm and z = 8 μm region if particle enters in the negative y or z directional force region, and there is no trapping on the first set of electrodes. After crossing the region between electrodes, an infected cell may reach in the negative y and

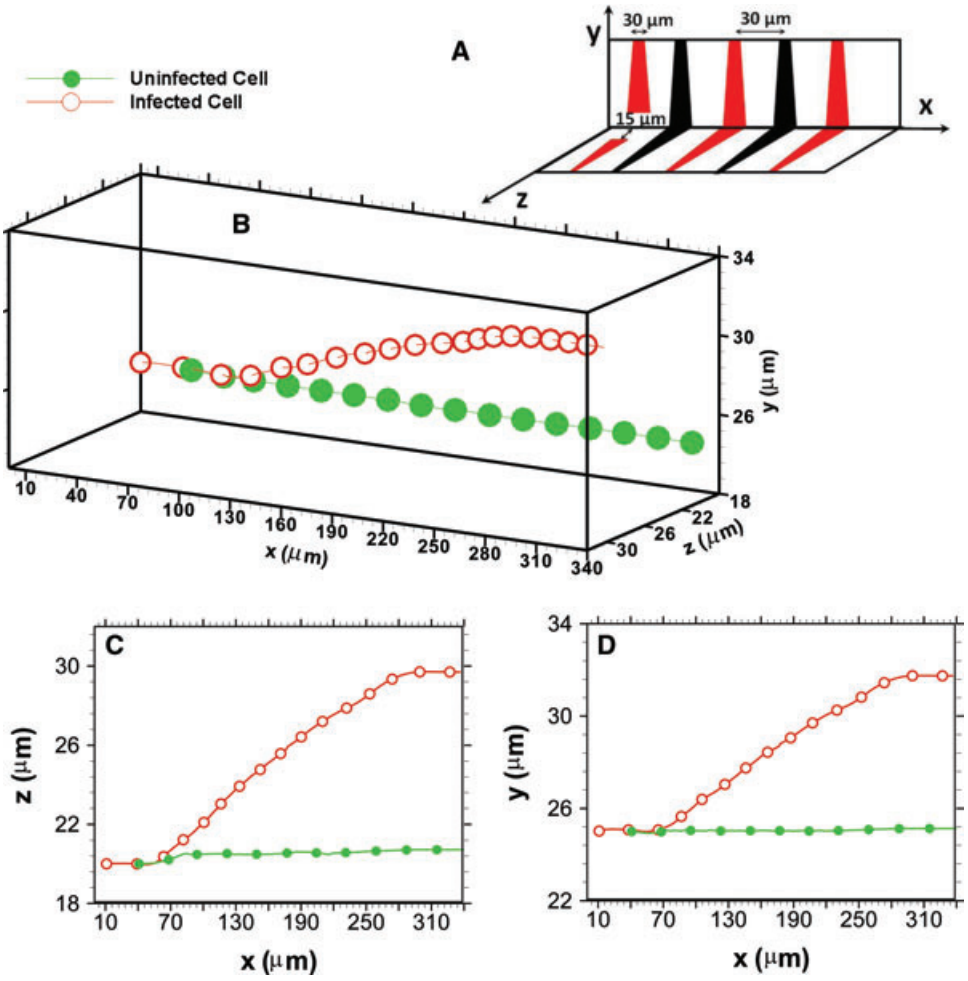

Figure 6. Effect of hybrid trapezoidal and periodic electrode configuration on cells' displacement in transverse and vertical directions. (A) schematic of electrodes' positions (B) translocation path of cells in actual domain, (C) projection of translocation path of particles on xz plane (D) projection of translocation path of particles on xy plane. The particles are considered simultaneously in the domain. RBCs and PF-infected RBCs were initially at the same y = 25 μm and z = 20 μm, but at different axial location (x = 40 and x = 10, respectively). The applied electric potential difference between a pair of electrodes is 10 $V_{p\text{-}p,}$ inlet fluid velocity is found from the flow field solution of main domain as shown in Fig. 1A. Here L = 400 μm and all other parameters are same as in Fig. 3.

z directional forcing region as shown in Fig. 5B. In such case, the negative y and z directional forces try to trap the cell toward the electrodes. However, the negative directional force competes with hydrodynamic force due to bulk fluid flow and positive x directional force component of dielectrophoretic force. Thus, the possibility of trapping to wall is much less in this configuration. Based on single cell simulation, hybrid configuration shows promise but the levitation of infected cell is around 16 μm and it is not sufficient for efficient separation of cells. Therefore, to increase the interparticle separation distance, we consider a combination of hybrid and periodic electrodes.

3.3 Separation of Cells

In this section, interparticle distances are reported for the combination of hybrid and periodic electrode configuration presented in Fig. 6A. Here, both cells are considered in the separation domain, and numerical simulation has been performed considering the presence of cells in the domain.

In the proposed microdevice (Fig. 1), the cells can enter the separation domain at any location in the y direction and within half width in the z direction due to fluid flow (not shown). For that reason, initially we consider uninfected and infected cells are at same y and z (y = 25 μm and z = 20 μm), but different locations in x direction (x = 40 and 10 μm, respectively). Figure 6C and D indicates that uninfected cell has very minor deviation from its path in both y and z directions, whereas infected cell displaces significantly in both the positive y and z directions. Therefore, uninfected cell will not travel further than z = 20 μm. That means the width of the outlets (in z direction) can be easily considered as 20 μm.

In the proposed configuration, while passing over the first set of electrodes, Fig. 5B indicates that a cell will try to reach at the line of y = 8 μm and z = 8 μm, if it stays below this line or inside the negative y and z directional force region above this line. Therefore, next we consider uninfected and infected cell at the same y and z (y = 8 μm and z = 8 μm), but different locations in x direction (x = 40 μm and 10 μm, respectively). Supporting Information Fig. 3(C) and (D) indicate that the difference in displacement/levitation between cells in z and y directions is the same, and the resultant interparticle distance in y and z directions is 18.14 μm, which is higher than that along these axes individually. Based on these

outcomes, it can be concluded that for any possible position of cells in the separation domain, the resultant interparticle distance due to two directional dielectrophoretic forces is higher than the conventional one directional force.

4 Concluding remarks

A new microdevice is presented to improve the efficiency of continuous separation of biological particles using AC DEP. The efficiency of separation is improved by implementing dielectrophoretic forces on particles in both transverse and vertical directions. RBC and PF-infected RBC are considered as sample cells in designing the microdevice. Different types of electrode configurations are used to achieve effective force on the cells. A hybrid configuration consisting of a set of trapezoidal electrodes and a set of truncated trapezoidal electrodes is found promising in increasing interparticle distance without any trapping on the electrode or channel wall. A full-scale numerical simulation indicates that a combination of hybrid and periodic electrodes can create sufficient dielectrophoretic forces in both transverse and vertical directions to increase the interparticle distance for improving the separation efficiency significantly. The proposed microdevice can be used for separation of different biological entities that have small difference in their dielectric properties (such as HIV infected cells and healthy cells) and that cannot be separated by conventional DEP device. The device design presented in this study is based on fixed electrode width and periodicity. This microdevice can be further optimized by undertaking a parametric study, and we plan to address that in a future work.

This work was partly supported by the National Science Foundation under Grant No. CTS 1250107.

The authors have declared no conflict of interest.

5 References

[1] Pohl, H. A., *Dielectrophoresis: The Behavior of Neutral Matter in Nonuniform Electric Fields*, Cambridge University Press, Cambridge, New York 1978.

[2] Morgan, H., Green, N. G., *AC Electrokinetics: Colloids and Nanoparticles*, Research Studies Press, PA 2001.

[3] Voldman, J., Gray, M. L., Toner, M., Schmidt, M. A., *Analyt. Chem.* 2002, *74*, 3984–3990.

[4] Markx, G. H., Huang, Y., Zhou, X. F., Pethig, R., *Microbiol.-UK* 1994, *140*, 585–591.

[5] Hu, X. Y., Bessette, P. H., Qian, J. R., Meinhart, C. D., Daugherty, P. S., Soh, H. T., *Proc. Natl. Acad. Sci. USA* 2005, *102*, 15757–15761.

[6] Doh, I., Cho, Y. H., *Sensor. Actuat. A-Phys.* 2005, *121*, 59–65.

[7] Li, Y. L., Kaler, K., *Anal. Chim. Acta* 2004, *507*, 151–161.

[8] Kralj, J. G., Lis, M. T. W., Schmidt, M. A., Jensen, K. F., *Anal. Chem.* 2006, *78*, 5019–5025.

[9] Cheng, I. F., Chang, H. C., Hou, D., *Biomicrofluidics* 2007, *1*, 021503.

[10] Han, K. H., Han, S. I., Frazier, A. B., *Lab Chip* 2009, *9*, 2958–2964.

[11] Khoshmanesh, K., Zhang, C., Tovar-Lopez, F. J., Nahavandi, S., Baratchi, S., Kalantar-Zadeh, K., Mitchell, A., *Electrophoresis* 2009, *30*, 3707–3717.

[12] Wang, L., Lu, J., Marukenko, S. A., Monuki, E. S., Flanagan, L. A., Lee, A. P., *Electrophoresis* 2009, *30*, 782–791.

[13] Choi, S., Park, J. K., *Lab Chip* 2005, *5*, 1161–1167.

[14] Wu, L. Q., Yung, L. Y. L., Lim, K. M., *Biomicrofluidics* 2012, *6*, 014113.

[15] Urdaneta, M., Smela, E., *Electrophoresis* 2007, *28*, 3145–3155.

[16] Braschler, T., Demierre, N., Nascimento, E., Silva, T., Oliva, A. G., Renaud, P., *Lab Chip* 2008, *8*, 280–286.

[17] Nascimento, E. M., Nogueira, N., Silva, T., Braschler, T., Demierre, N., Renaud, P., Oliva, A. G., *Bioelectrochemistry* 2008, *73*, 123–128.

[18] Gascoyne, P., Pethig, R., Satayavivad, J., Becker, F. F., Ruchirawat, M., *Biochim. Biophys. Acta* 1997, *1323*, 240–252.

[19] Voldman, J., Toner, M., Gray, M. L., Schmidt, M. A., *J. Electrostat.* 2003, *57*, 69–90.

[20] Iliescu, C., Yu, L. M., Tay, F. E. H., Chen, B. T., *Sensor. Actuat. B-Chem.* 2008, *129*, 491–496.

[21] Durr, M., Kentsch, J., Muller, T., Schnelle, T., Stelzle, M., *Electrophoresis* 2003, *24*, 722–731.

[22] Chen, D. F., Du, H. J., *Microfluid. Nanofluid.* 2007, *3*, 603–610.

[23] Park, S., Zhang, Y., Wang, T. H., Yang, S., *Lab Chip* 2011, *11*, 2893–2900.

[24] Kuczenski, R. S., Chang, H. C., Revzin, A., *Biomicrofluidics* 2011, *5*, 032005.

[25] Sharma, N., Patankar, N. A., *J. Comput. Phys.* 2005, *205*, 439–457.

[26] Wang, X. J., Wang, X. B., Gascoyne, P. R. C., *J. Electrostat.* 1997, *39*, 277–295.

[27] Jubery, T. Z., Prabhu, A. S., Kim, M. J., Dutta, P., *Electrophoresis* 2012, *33*, 325–333.

[28] Shim, J., Dutta, P., Ivory, C. F., *Numer. Heat Tr. A-Appl.* 2007, *52*, 441–461.

[29] Jubery, T. Z., Dutta, P., *Numer. Heat Tr. A-Appl.* 2013, in press.

[30] Heinrich, V., Ritchie, K., Mohandas, N., Evans, E., *Biophys. J.* 2001, *81*, 1452–1463.

[31] Mernier, G., Piacentini, N., Braschler, T., Demierre, N., Renaud, P., *Lab Chip* 2010, *10*, 2077–2082.

